Data Fusion of Four ABS Sensors and GPS for an Enhanced Localization of Car-like Vehicles

Philippe Bonnifait, Pascal Bouron, Paul Crubillé, Dominique Meizel

Heudiasyc UMR CNRS 6599
Université de Technologie de Compiègne. France.
Philippe.Bonnifait@hds.utc.fr

Abstract

A localization system using GPS, ABS sensors and a driving wheel encoder is described and tested through real experiments. A new odometric technique using the four ABS sensors is presented. Due to the redundancy of the measurements, the precision is better than the one of differential odometry using the rear wheels only. The sampling is performed when necessary and when a GPS measurement is performed. This implies a noticeable reduction of the GPS latency, simplifying thus the data-fusion process and improving the quality of its results.

1 INTRODUCTION

Real-time continuous localization is essential for many applications concerning outdoors vehicles [6-1-9]. It consists of estimating the vehicle location in a global digital map. GPS is a very attractive solution because it is affordable and convenient. Moreover, since May 2000, the SA degradation has been turned off, and the natural precision (a few meters) is sufficient for usual navigation tasks. Nevertheless, GPS still suffers from satellite masks occurring in urban environments, under bridges, tunnels or in forests. GPS appears then as an intermittent positioning system that demands the help of a dead-reckoning system. Commercially available solutions use an odometer, a gyro and sometimes a magnetic compass [1] to maintain an estimation of the position during satellites masks. On the other hand, braking in modern cars is assisted with ABS systems that utilize angular encoders attached to the wheels. In this case, the sensors basically measure the wheel speeds. We propose hereafter to use them to estimate traveled distances.

This paper presents a new odometric technique that can advantageously replace the commercially available dead-reckoning techniques that use supplementary sensors like gyros [2]. The models presented in the sequel are real odometric models and not discretized kinematics models like in [7]. Assumptions are made on the elementary motions and geometric relationships are expressed to provide relations between the rotations of the wheels and the displacements.

The paper is organized as follows: section 2 describes an odometric technique using four ABS sensors together with an encoder measuring the driving wheel angle. The fusion of all these measurements uses an Extended Kalman Filter. A special attention is dedicated to the sampling process that is customized to the GPS. This is done by taking both the displacement and the time as progression variables. Experiments show the efficiency of this technique in comparison with differential odometry using only the sensors of the rear wheels. The complete localizer in then presented in section 3. Experiments performed with a laboratory car quantify the precision obtained when the GPS is available and when satellite masks occur.

2 ODOMETRY WITH ABS SENSORS

The purpose of odometry is to build an incremental model of the motion using measurements of the elementary wheel rotations. In this section, we first introduce the generic integration process whose inputs are theoretical quantities (not directly measured). In a second time, these inputs are estimated using the measurements of all the encoders. This is one major contribution of the paper, the second one being the sampling strategy.
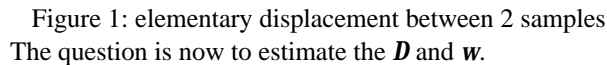
2.1 Integration process

Consider a car-like vehicle (figure 2). The mobile frame M is chosen with its origin M attached to the center of the rear axle. The x-axis is aligned with the longitudinal axis of the car. At time t_k, the vehicle position is represented by the (x_k, y_k) Cartesian coordinates of M in a world frame W. The heading angle is denoted $\boldsymbol{q}_k$.

Let M_k and M_{k+1} be two successive positions. Supposing the road is perfectly planar and horizontal, as the motion is locally circular, we have (figure 1):
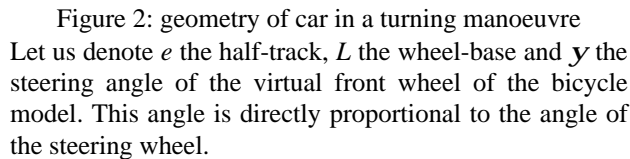
$$\Delta = \rho.\omega \tag{1}$$

where $\boldsymbol{D}$ is the length of the circular arc followed by M, $\boldsymbol{w}$ the elementary rotation of the mobile frame, and $\boldsymbol{r}$ the radius of curvature and I the instantaneous center of rotation.

Supposing the car is moving forward, the variation on the position is expressed as:

$$\begin{cases} \boldsymbol{D}x & = & |\boldsymbol{M}_k\boldsymbol{M}_{k+1}|.cos(\boldsymbol{q}_k + \boldsymbol{w}/2) \\ \boldsymbol{D}y & = & |\boldsymbol{M}_k\boldsymbol{M}_{k+1}|.cos(\boldsymbol{q}_k + \boldsymbol{w}/2) \end{cases}$$

From basic Euclidean geometry, we know that $\{D \approx |M_k M_{k+1}|\}$ up to the second order. The integration process is then:

$$\begin{cases} x_{k+1} & = & x_k + D.cos(q_k + w/2) \\ y_{k+1} & = & y_k + D.sin(q_k + w/2) \\ q_{k+1} & = & q_k + w \end{cases} \qquad (2)$$

Figure 1: elementary displacement between 2 samples

The question is now to estimate the D and w.

2.2 Estimating D and w

Consider the four wheels vehicle sketched on figure 2.

Figure 2: geometry of car in a turning manoeuvre

Let us denote e the half-track, L the wheel-base and y the steering angle of the virtual front wheel of the bicycle model. This angle is directly proportional to the angle of the steering wheel.

In order to develop an odometric model, we assume that, between two samples, the wheels do not slip and that the distances e and L are known and constant: this is a simplified view of the phenomenon occurring at the tire/ground contact zone.

D and w can be estimated using the steering angle y and the elementary distances traveled by each wheel. In the sequel, D_{RL} and D_{RR} denote the distances traveled between two samples by the rear wheels and D_{FL} and D_{FR} those traveled by the front wheels.
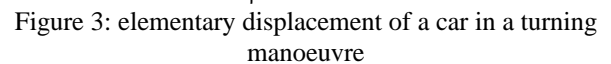
Observation equation

The driving wheel encoder (which measures ψ) provides a relation between D and w. Figure 2 gives:

$$\tan(y) = \frac{L}{r} \qquad (3)$$

Rewriting equations (1) and (3):

$$\tan(y) = L.\frac{w}{D} \qquad (4)$$

Let consider the situation described in figure (3). Since the rear wheels do not turn, we directly have:

$$D_{RL} = w.(r\text{-}e) = D\text{-}e.w \qquad (5)$$

$$D_{RR} = w.(r\text{+}e) = D\text{+}e.w \qquad (6)$$

Figure 3: elementary displacement of a car in a turning manoeuvre

Commonly, in the technique called *differential odometry* [9], D and w are computed just using the measurements (D_{RR}, D_{Rl}):

$$D = \frac{D_{RR} + D_{RL}}{2} \quad w = \frac{D_{RR} - D_{RL}}{2.e}$$

The measurements of the front wheels are more difficult to use because their orientation with respect to the mobile frame is not constant. In order to simplify, let consider the virtual front wheel. The length of the circular arc it follows between two samples is (Fig 3):

$$D_F = D.w$$

Now,

$$D = \frac{L}{\sin(y)}$$

By using (3), we have:

$$D = \frac{r}{\cos(y)}$$

By multiplying each side by w:

$$D_F .\cos(y) = D \qquad (7)$$

The same procedure can be applied to each front wheel; it yields (y_L and y_R are shown on figure 2):

$$\tan(y_L) = \frac{L}{r\text{-}e} \text{ and } \tan(y_R) = \frac{L}{r\text{+}e}. \qquad (8)$$

r can be eliminated in (8) by using relation (3). One gets:

$$y_L = \text{atan}\left(\frac{\tan(y).L}{L\text{-}e.\tan(y)}\right) \text{ and } y_R = \text{atan}\left(\frac{\tan(y).L}{L\text{+}e.\tan(y)}\right) \qquad (9)$$

Finally, the adaptations of equation (7) for each wheel are:

$$D_{FL}.\cos(y_L) = D\text{-}e.w \qquad (10)$$

$$D_{FR}.\cos(y_R) = D\text{+}e.w \qquad (11)$$

Equations (4, 5, 6, 10, 11) define a redundant and non-linear system that links the unknown quantities (D, w) to the measured variables (D_{FL}, D_{FR}, D_{RL}, D_{RR}, y):

$$\begin{cases} \tan(y) & = & L.\dfrac{w}{D} \\ D_{RL} & = & D\text{-}e.w \\ D_{RR} & = & D\text{+}e.w \\ D_{FL}.\cos(y_L) & = & D\text{-}e.w \\ D_{FR}.\cos(y_R) & = & D\text{+}e.w \end{cases} \qquad (12)$$

Defining an equivalent measurement vector (13), equation (12) takes the usual form of observation equation (14).

$$z = [\tan(y), D_{RL}, D_{RR}, D_{FL}.\cos(y_L), D_{FR}.\cos(y_R)]^{T} \qquad (13)$$

$$z = h(z) \qquad (14)$$

State estimation of (D, w)

Because of presence of unavoidable slippage and modeling errors, we propose to use all the measurements to estimate the state vector $z=[D, w]^{T}$. The redundancy should reduce the effects of the unknown disturbances.

Since the observation equation (14) is not linear, we propose to apply an Extended Kalman Filter (EKF), interpretable here as a Weighted Least Squares estimator. This technique presents also the advantage to estimate the covariance of the estimation error, which will be useful for further estimating the localization $[x, y, q]^{T}$ by EKF.

Since the models we use are odometric ones and that no acceleration nor forces are supposed to be known, the variation of the state vector is modeled by a Wiener process whose input g_k is a zero-mean white noise with a Q_g covariance matrix:

$$z_{k+1} = z_k + g_k$$

Since the equivalent measurements that are the components of z (eq. 13) are obtained from five different sensors, we can assume that the covariance matrix R of z is diagonal. The EKF estimation can therefore be split into five independent computations, each one involving a scalar division in place of inverting a 5x5 matrix.

Denote S the variance of the estimation error. The EKF works in six steps:

Prediction stage

$$S_{k+1/k} = S_{k/k} + Q_\gamma$$

Estimation stages

1) As the first observation equation is not defined when D equal zero (see eq. 13), we only use it when the speed of the car is high enough.

Moreover, this equation being non-linear, we compute the Jacobian matrix with respect to the state:

$$C_1 = \left[\frac{dz_1}{dz}\right] = \left[\begin{array}{cc} \dfrac{\text{-}L.w}{D^2} & \dfrac{L}{D} \end{array}\right]$$

The updated state and variance matrix are then given by:

$$K_k = S_{k+1/k}.C_1^{t}.(C_1.S_{k+1/k}.C_1^{t}+R_2)^{-1}$$

$$z_{k+1} = z_k + K_k.(z_2 - C_1.z_k)$$

$$S_{k+1/k+1} = (I_{22} - K_k.C_1).S_{k+1/k}$$

2) The four other observations provide estimations as follows:

for i=2 to 5,

$$C_i = [1 \; +/\text{-}e]$$

$$K_k = S_{k+1/k+1}.C_i^{t}.(C_i.S_{k+1/k}.C_i^{t}+R_i)^{-1}$$

$$z_{k+1} = z_{k+1} + K_k.(z_i - C_i.z_{k+1})$$

$$S_{k+1/k+1} = (I_{22} - K_k.C_i).S_{k+1/k+1}$$

end for.

Finally, each estimation of (D, w) is used in the model (2) to provide an odometric location (starting from a given position and heading). This technique is called odometric EKF in the sequel.

2.3 Sampling the odometric EKF

Commonly, odometric models are sampled with respect to time. One should notice that they can be sampled with respect to the traveled distance. As a matter of fact, the sampling rate must be such that the elementary motion is circular. Actually, as long as the steering angle is constant, the motion is circular. Therefore, the model should be sampled when a significant variation of the steering angle is detected during a displacement.

This sampling strategy presents also the interest to be well adapted to the physical nature of the process: if the car is motionless, the model is not sampled and the estimation error logically does not increase.

On the other hand, the position *(x, y)* in the model (2) is not observable [3] from the encoder measurements (13). One can use a GPS receiver to correct the unavoidable drift of the odometric EKF. This is nowadays an affordable sensor, but its latency can induce unacceptable errors when the speed is high. The GPS latency is the delay between the moment all the visible satellites measurements are performed and the moment the position is output and received by the onboard computer. The transmission delay is unavoidable but the latency can be reduced to its minimum by using the analogous signal "1PPS" available on the Motorola VP ONCORE used in

our experiments. This signal rises each time the satellites are sampled. Thus, we propose to trig the odometric EKF using the "1PPS" signal.

In summary, the sampling is performed as following:
- each time a GPS measurement is performed,
- each time the car has traveled one meter **and** the steering angle has changed more than 0.5 degree.

The two sampling processes are asynchronous. The sampling frequency is not constant and higher than 1Hz. It can reach several Hz while entering in a roundabout for example.

2.4 Tuning of the filter

For the car used in the experiments (a Citroën Xantia Break see photo on figure 4), the sources of errors that affect the observation (14) are numerous. The first ones result from the resolutions of the ABS encoders (1.93 cm for D_{RL}, D_{RR}, D_{FL}, D_{FR}) and of the driving wheel encoder ($2.\pi/4096$ rad for y). The other ones are due to the approximate nature of the model (12) (for instance, distances e and L are not exactly constant).

Since there are several uncorrelated causes of error, we can suppose that inaccuracy can be globally represented by an additive zero-mean temporally uncorrelated noise.

Figure 4: the car used in the experiments

In order to tune the EKF, we have computed position errors in comparison with a post-processed DGPS. The tuning of the filter is assumed to be correct when the errors are consistent with the 3σ bounds (99% of confidence bounds).

2.5 Results of the odometric EKF

The experimental results presented in this section were obtained using stored data of the sensors. The sampling of the odometric EKF has been done has presented in section 2.2.3. The rough measurements of the GPS receiver VP ONCORE were stored and then processed in association with a fixed receiver in order to produce the *true* positions of the car (Kinematic Differential GPS on L1 with the software *Jupiter*). The precision is estimated to be better than two meters while the car is moving.

The initial heading has been computed with an error less than 0.5 degrees.

The odometric EKF has been tested on four laps of 2.4 km long, at the maximum allowed speed of 50 km/h. Results are shown on figure (5) (thick line) and compared

with differential odometry using rear wheels only (dotted lines) and with the true trajectory (thin line).
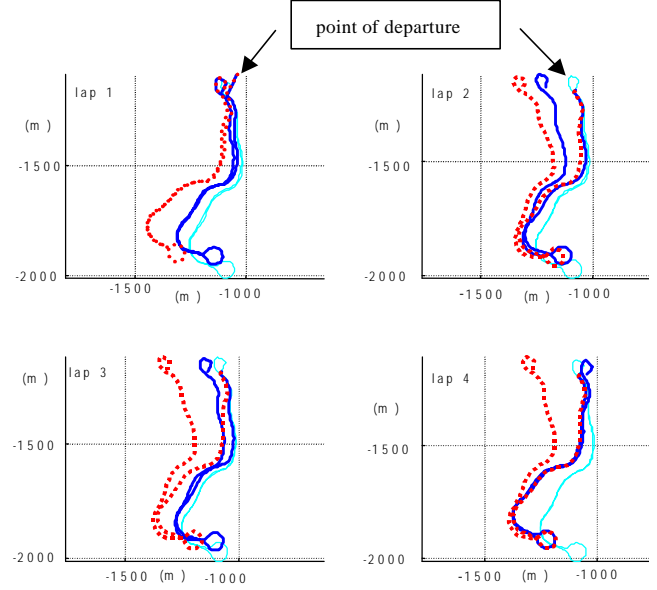

Figure 5: tops views of the experiments

Figures (6) and (7) show longitudinal and lateral errors (with respect to the DGPS) as functions of the linear abscissa, making the benefit of the odometric EKF clearer.

It can be seen from these plots that the use of all the sensors increase significantly the precision. This can be explained by the fact that the redundancy in average allows a better estimation. For example, slips which disturb the front wheels may not affect the rear ones.

Moreover, other experiments, not reported here, have shown that the drift of the estimation of the heading of the odometric EKF is in the same order as the one of a dead-reckoning technique using an odometer and a vibrating gyro (a British Aerospace VSG2000).
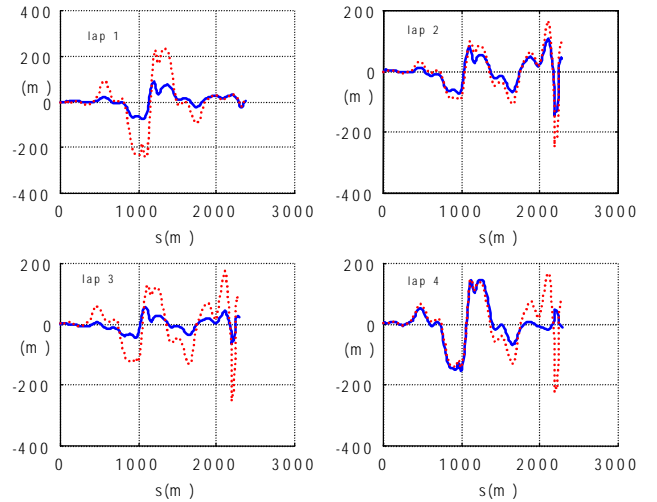

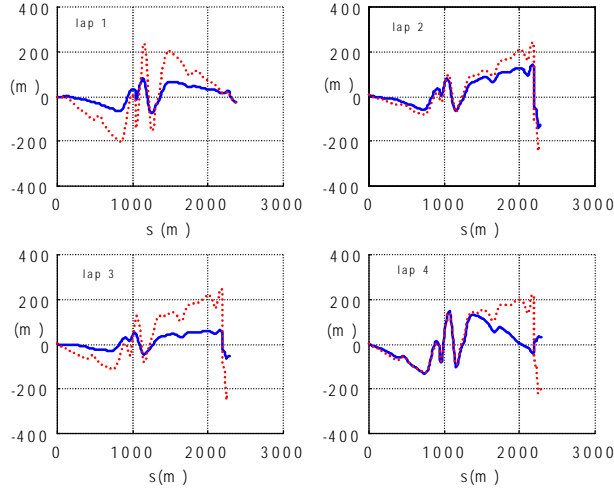Figure 6: longitudinal errors as functions of the distance

Figure 7: lateral errors as functions of the distance

3   SENSOR FUSION OF GPS AND ODOMETRY

When a GPS position is available, a correction of the odometric estimation is performed using an Extended Kalman Filter formalism with noisy input.

3.1   Architecture

The odometric EKF computes an estimation of $z=(D, w)$ and of the covariance matrix S. This data is used as the input of a second EKF estimating (x,y,θ). The measurements (x,y) of the GPS (in a local ground frame) are used as the observations. It is obvious that the GPS data change with the number of visible satellites. One usual way to take into account this non stationarity consists to inflate the state covariance matrix each time the constellation changes.
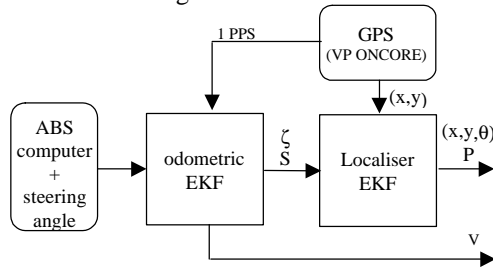

Figure 8: architecture of the localization system

This architecture can be seen as a "loosely coupled fusion system" [8].

3.2   Heading observability

The heading q is not directly measured since the GPS is used as a position sensor. Nevertheless, by studying the state observability of the non linear system [3], it is easy to verify that the observability condition is verified when the speed of the car is non-zero.

In order to assess what happens in this case, let consider a car when it stops: the measurement w becomes zero without any noise (no signal come from the ABS encoders) and the odometric prediction of the heading

does not change. This is interesting when compared with a dead reckoning system using a gyro that will suffer from drifting in the same condition. When the vehicle will move again, the localizer will start with a non detoriorated estimation of the heading.

3.3   Tuning of the filter

The errors on position measured by GPS (with the SA degradation off) are temporally correlated. We have estimated a first order Auto-Regressive model [5] of the noise. The time-constant of this AR model is approximately 2 hours [4]. This value exceeds the time-constant desired for the filter from several degrees of magnitude. It is thus not good to define an augmented state that incorporate this AR model.

One practical solution to take into account the correlation of the noise consists to increase the variances of the observations. If not, the filter would yield erroneous too confident estimations [4]. In the experiments presented in the sequel, we have supposed that the variances Rx and Ry of the observations were constant and, experimentally, we have used a 5 ratio for the augmentation ($Rx=5*1.22^2$ m and $Ry=5*2.75^2$ m). The first rough GPS measurement is used to initialize the position.

3.4   Results

The global localizer has been tested on the four laps of the experiment of section 2.5 (9.6 km long run). Errors are computed thanks to the post-processed DGPS.

Three characteristics are tested in this experiment:

1) The normal operation with all measurements available,
2) seven small GPS masks of ten seconds (for $70<t<210$ s), similar to the ones observed in town circuits,
3) a large one of 5 minutes (for $900<t<1200$ s) to test the robustness of the error computation.

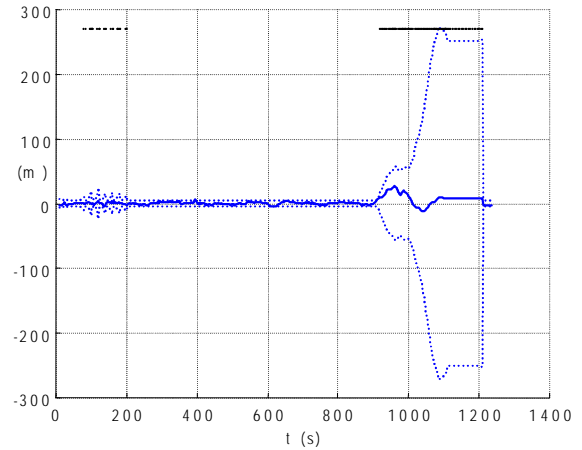Figures 9, 10, 11 and 12 present the results (the dotted lines are the 3 σ estimated bounds).

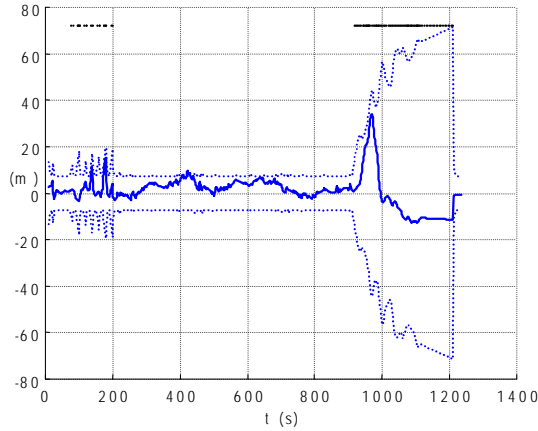Figure 9: x error and 3 σ estimated bounds

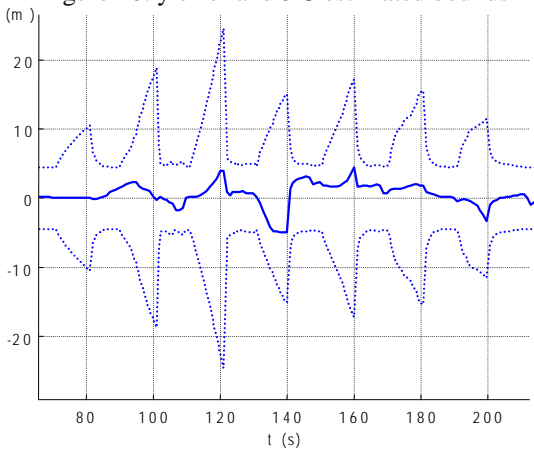Figure 10: y error and 3 σ estimated bounds

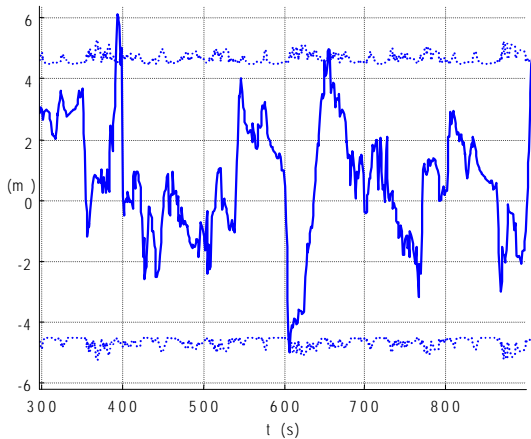Figure 11: x error during the small masks

Figure 12: x error when the GPS is ok.

Even if they are computed using a linearized model, the large mask shows that the errors are well estimated since the confidence bounds are consistent with the errors (figures 9 and 10).

Figures 11 and 12 focus on interesting parts of figure 9. On figure 11, it should be noticed that, each time a mask occurs, the error is consistent with the estimated confidence. This realistic situation gives an idea of the actual precision (a few meters) of the localization.

Figure 12 indicates that the tuning of the filter is well done since the estimated 3 standard deviation is consistent with the error. Naturally, the position error is mainly the one of the GPS and therefore is not white.

4   CONCLUSION

This work has presented the development of a localization system and its experimentation with real data. It is a very cheap localizer, since it uses natural GPS receiver and ABS sensors available on most modern cars. Thanks to an adequate sampling, the proposed odometric method is computed when necessary and in a way well adapted to a GPS correction. The experiments have proved that the use of all the ABS sensors increases the precision of the positioning system in comparison with the use of only the two ones associated with the rear wheels. This dead-reckoning technique is sufficient to maintain a precise estimation of the position during small GPS masks. During large masks, we think it will produce an efficient estimation of the local trajectory which should be useful for the map-matching process with a precise digital map. The future work concerns the study of an automatic calibration of the wheels circumference. As a matter of fact, even it not very sensible to the variation of tires pressure, the circumference changes with the wear of the tires.

References

[1] E. Abbott and D. Powell. "Land-Vehicle Navigation using GPS". Proc. of the IEEE, Vol. 87, NO. 1, Jan. 99.

[2] B. Barshan and H.F. Durrant-Whyte. "Inertial navigation systems for mobile robots". IEEE Trans. on Rob. and Auto. Vol. 11, n°3, June 95. pp. 328-342.

[3] Ph. Bonnifait, G. Garcia. "Design and Experimental Validation of an Odometric and Goniometric Localization System for Outdoor Robot Vehicles". IEEE Trans. on Rob. and Auto. Vol. 14, n° 4, 98, pp. 541 - 548.

[4] Ph. Bonnifait, P. Bouron. "Statistical Modeling of the GPS and DGPS signals". Technical report UTC/Heudiasyc, n° 2296. May 2000.

[5] S. Cooper and H. Durrant-Whyte. "A Kalman Filter Model for GPS Navigation of Land Vehicles". IROS. Sept. 94. Munich. pp. 157-163.

[6] J. Guivant, E. Nebot, S. Baiker. "High accuracy Navigation Using Laser Range Sensors in outdoors Applications". ICRA2000. San Francisco. pp. 3817-3822.

[7] S. Julier, H. Durrant-Whyte. "Process Models For The High-Speed Navigation of Road Vehicles". ICRA. 1995. pp. 101-105.

[8] D. Mc Neil. "Multi-rate Sensor Fusion for GPS Navigation Using Kalman Filtering". M. Sc. Report. Virginia Polytechnic Institute. May, 99.

[9] Y. Zhao. "Vehicle Location and Navigation Systems". Artech House. 1997.